ChemComm

Cite this: *Chem. Commun.*, 2012, **48**, 11748–11750

www.rsc.org/chemcomm

COMMUNICATION

Electrical pulse triggered reversible assembly of molecular adlayers†

Shern-Long Lee,*[a] Yu-Ju Hsu,[a] Hung-Jen Wu,[a] Hsing-An Lin,[b] Hsiu-Fu Hsu*[b] and Chun-hsien Chen*[a]

Received 26th July 2012, Accepted 18th October 2012
DOI: 10.1039/c2cc35413f

Reversible adlattice assembly for alkoxy-decorated aromatics is controllable by short electrical pulses.

The control over molecular patterning is of fundamental and contemporarily technological significance.[1–3] Among the bottom-up approaches which hierarchically organise supramolecular architectures in two or three dimensions, the most prevalent method is molecular self-assembly which develops spontaneously *via* subtle intra/intermolecular interactions.[4] For phenomena taking place at the liquid–solid interface, the monolayer assembly can be further tailored by strategies including dewetting,[5] zone casting,[6] shear flow,[7] and electrochemical treatment.[8,9] STM (scanning tunnelling microscopy) is a powerful characterisation tool which can resolve the adlayer structure down to the molecular level[2,3] and, moreover, can unravel structural development in response to external stimuli, for example, by electrochemical control[8,9] or photo-irradiation.[9,10] In principle, external electrical stimuli can be readily delivered by STM tips. Examples such as pulse-induced desorption,[11] monolayer re-assembly,[12] and polymerisation[13] have been reported. Herein, we look into the effect of electrical pulses on physisorbed structures of hexakis((3,4-bi-(dodecyloxy)phenyl)-ethynyl)benzene (**1**, Fig. 1). The discotic nematogenic core favours a columnar mesophase and the alkoxy side chains develop molecular swirls in the liquid-crystalline phase and hexagonal monolayers at the liquid–solid interface.[14] The monolayers of **1** are employed in the present study to demonstrate that the application of short electrical pulses (3–8 V per 10 μs) *via* the STM tip is a convenient yet unexplored approach to reversibly generate molecular patterns from hexagons to honeycomb nanopores in a controllable manner.

Fig. 1 manifests the effect of 10 μs electrical stimuli on the transformation of molecular adlattices. The sample was prepared by placing a drop of phenyloctane containing 1 μM **1** on HOPG (highly oriented pyrolytic graphite). Fig. 1a displays a typical STM image and the proposed structure for the self-assembled adlattice. The alkoxy chains and the discotic core with seven phenyl rings can be unambiguously identified. The peripheral alkoxy chains swirl counter-clockwise toward the centre of **1**. There are domains exhibiting the other swirl direction (not shown). The detailed analysis of the structure was reported recently.[12] Similar to many monolayer systems of alkyl-decorated aromatics, some of the alkoxy side chains of **1** are unobserved, ascribed to being fluxional in solution as what was generally proposed in literature studies.[2] The formation of the hexagonal structure takes place spontaneously and, somewhat surprisingly, the assembly may also be expedited by a pulse of 3 V (the sample is grounded). By applying a subsequent pulse of 4 V, the imaging details of the alkoxy side chains of **1** are lost (Fig. 1b). With another pulse of 5 V, the adlattice becomes a nanoporous network (Fig. 1c); without the 5 V pulse, the assembly of the nanopores would otherwise not develop spontaneously even in days after **1** is dropcast on HOPG. The formation of nanopores also takes place in solvents such as octane, 1,2,4-trichlorobenzene, and *n*-tetradecane, but not at the solid–gas interface (Fig. S2, ESI†). For the concentration of **1** being as low as 1 nM, a 5 V pulse in phenyloctane results in an incomplete nanoporous structure (Fig. S3, ESI†).

To correlate the structure of the underlying layer with the adlattice, reduced tunnelling impedance is utilised such that the tip penetrates into the molecular assembly and thus unveils the structure of substrate or the strongly adsorbed first layer.[2,3] The resulted hexagonal structures similar to that shown in Fig. 1a are observed for the metastable bilayer (*vide infra*) and the nanopore motifs (Fig. S6, ESI†), suggesting that a pulse of 4 V per 10 μs introduces, on top of the underlying hexagons, a second layer of **1** which is repositioned to the molecular interstice of the first layer after a 5 V pulse. The observations are also true for 1 and 100 μs pulses. It is noteworthy that, without electrical stimuli, the structural conversion between hexagons and honeycomb nanopores has never been observed within the experimental time span in hours, indicating that both lattices are thermodynamically stable.

To associate the adlattice structure with the magnitude of pulse potentials, Fig. 2 displays consecutive frames acquired upon the sample being subjected to electrical stimuli. The voltages of the applied sequence are 5, 4 V, and followed by 5, 4, 3 V. Panels b and e show that a 5 V pulse always generates honeycomb nano-pores regardless of whether the pulse is applied to the hexagonal monolayer (panels a and b) or to the bilayer (panels d and e), generated from 3 or 4 V pulses, respectively. Panels g–i show that applying a pulse sequence with a descending order of voltages at the honeycomb

[a] *Department of Chemistry and Centre for Emerging Material and Advanced Devices, National Taiwan University, Taipei, 10617, Taiwan. E-mail: sllee@ntu.edu.tw, chhchen@ntu.edu.tw; Fax: +886 02-2363-6359*
[b] *Department of Chemistry, Tamkang University, Taipei, 25137, Taiwan. E-mail: hhsu@mail.tku.edu.tw; Fax: +886 02-2620-9924*

† Electronic supplementary information (ESI) available: Experimental details, STM images acquired as a function of tunnelling impedance, solvents, and concentrations of **1**. See DOI: 10.1039/c2cc35413f

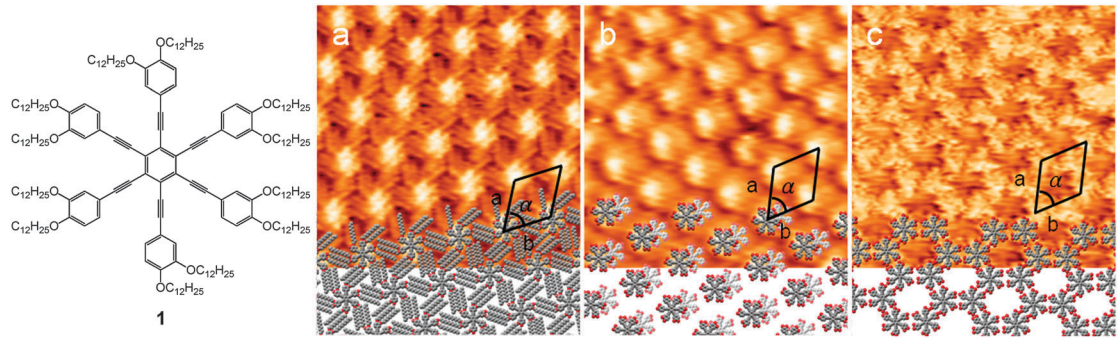

Fig. 1 Structure of hexakis((3,4-bis(dodecyloxy)-phenyl)ethynyl)benzene, **1**, and STM images of **1** after the application of 10 μs pulses of (a) 3 V, (b) 4 V, and (c) 5 V which result in, respectively, characteristics of a hexagonal monolayer, a bilayer, and a honeycomb motif. For clarity, the alkoxy side chains illustrated in panel a are not shown in panels b and c (red indicates oxygen atom). Unit cell parameters of $|\vec{a}|$, $|\vec{b}|$, and α: (a) 3.4 (±0.2) nm, 3.3 (±0.2) nm, 60° (±2°); (b) 3.2 (±0.3) nm, 3.2 (±0.2) nm, 62° (±2°); (c) 3.4 (±0.2) nm, 3.3 (±0.3) nm, 60° (±3°). Their unit cell vectors are indistinguishable for these structures and panel c has an additional molecule in the unit cell. Conditions: solutions, 1 μM **1** in phenyloctane; image acquisition, 30 s per frame; E_{bias}, 0.8 V; $i_{tunnelling}$, 60 pA. Image size: 18 × 18 nm.

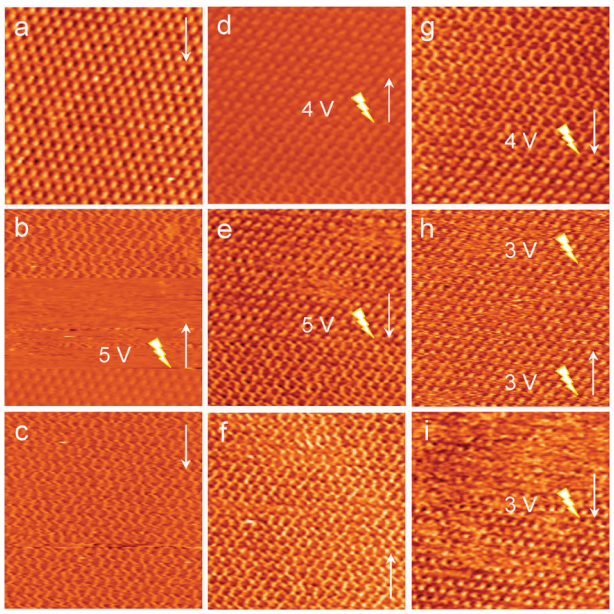

Fig. 2 Consecutive STM images for real-time monitoring of the molecular assembly in response to electrical pulses. The applied voltages and the scan directions are indicated in the images. Image size: 40 nm × 40 nm; image acquisition, 30 s per frame. Other conditions are the same as those in Fig. 1. The blur portion in panel b was due to the feedback response to an adjacent protrusion which was confirmed by examining a larger scan area after the imaging sequence was finished. Subsequent images appear unaffected by the protrusion, attributed to the thermal drift of the piezoelectric scanner.

nanopores also gives rise to the bilayer with a 4 V pulse and hexagons with 3 V pulses. Note that the pulse sequence is reversed from that shown in Fig. 1. To obtain the hexagonal monolayer *via* the bilayer structure, it sometimes requires a few 3 V pulses to expedite the structural conversion, indicative of desorption and re-adsorption of **1** upon the treatment of 3 V pulses. For example, it took three 3 V pulses (panels h and i) to acquire a hexagonal monolayer as shown in Fig. 2i. The formation of hexagons directly from honeycomb nanopores by the use of 3 V pulses is unsuccessful yet, by taking a 4 V pulse to route through the bilayer intermediate, the nanopores can always be transformed into the hexagonal monolayer, suggesting that the energy barrier for the structural transformation is overcome or reduced by the electrical stimuli.

With a pulse of 6–8 V per 10 μs to the honeycomb nanopores, the image immediately shows bare HOPG, indicative of desorption of the molecules. The hexagonal monolayers of **1** re-assemble in about 1 h, similar to that required for the spontaneous formation of monolayers from dropcast films. A harsh stimulus larger than 8 V generally damages the substrate and results in a rugged morphology. It is worth noting the effect of oppositely biased pulses, in which the tip potential is negative against that of the substrate. For a pulse bias of −1 V and −2 V, the structure of honeycomb nanopores remains unaffected. With a stronger pulse, such as −3, −4, and −5 V, the surface exhibits characteristics of HOPG. Although the substrate is grounded, there is an electric double layer at the solid–liquid interface. The pulses trigger charging/discharging events such that the adsorbed **1** experiences residual positive potential and thus becomes destabilised. Taking together, the adlattice structure is primarily determined by the applied voltage and fairly independent of the structure prior to the pulse. Each stimulus concomitantly redistributes the developed local charge at the solid–liquid interface and results in the assembly associated well with the voltage magnitude. Considering the fact that the assembled molecules can be driven away by a pulse of −3 to −5 V at the tip, it is reasonable to hypothesise that the desorption involves electrostatic repulsion or that the adsorbed **1** may be polarised with positive charge in contact with the substrate. Therefore, the following mechanism is proposed to explain the controllable formation of the molecular patterns. The electrical pulse discharged at the STM tip polarises **1** which subsequently is attracted to a complimentarily polarised site on the substrate. On the first layer, the aromatic core bears a relatively larger polarisability than those of the alkoxy chains. Consequently, a 4 V pulse may furnish the effective charge primarily localised at the aromatic core of the very first layer and yields a bilayer configuration. For a larger applied voltage, the difference in the effective charge over the alkoxyl and aromatic moieties is less significant such that the enthalpic factors to

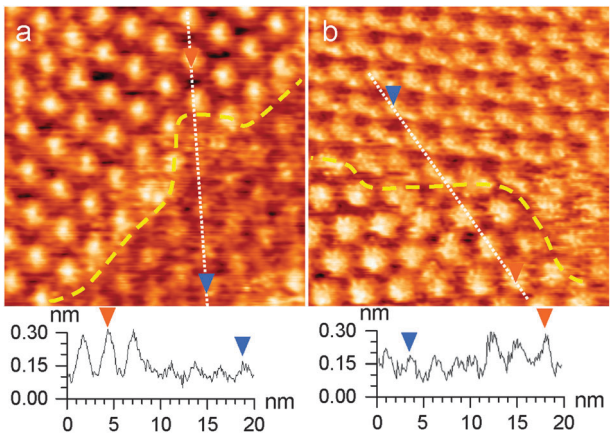

Fig. 3 Differences in apparent heights between domains of (a) monolayer and bilayer, (b) bilayer and nanoporous structures. Lower panels are cutaway views of the white dotted lines shown in the images in which the orange triangles indicate the bilayer structure. E_{bias}, 0.65 V; $i_{tunnelling}$, 60 pA. Image size: 24 × 24 nm.

maximise the adsorbate coverage dominate and thus the adlattice adopts honeycomb arrangement with a 5 V pulse. In addition, relatively high local concentration and local heating upon the electrical stimuli should facilitate the structural transformation.

Electrical pulses in STM studies are generally applied to recover the tip performance by expelling adsorbed contaminants away from the tip. Very recently, we indeed demonstrated that, for an STM tip pre-coated with target molecules, dibenzo[*g*,*p*]-chrysene (DBC), isolated DBC can be deposited onto the substrate with a pulse of 7 V per 10 μs in an environment purged with dry nitrogen or in a DBC-free solution of phenyloctane.[15] Similarly, in the present study molecules adjacent to the STM tip experience the electrical field and have the tendency to be ejected toward the substrate. The pulse-triggered molecular patterns are thus expected to be proximal to the tip. Accordingly, it is important to look into whether the domain size of the honeycomb nanopores is strongly associated with the strength of the applied electrical field. This parameter can be tuned by the tip–substrate distance (Fig. S9, ESI†) and by the addition of electrolytes to the solution (Fig. S10, ESI†). By applying a 5 V per 10 μs pulse to the hexagonal monolayer, the domain size of nanopores is about 500 nm. By retracting the tip away from the imaging position for 1–5 nm and 20 nm, the domain size is reduced to *ca.* 250 nm and 50 nm, respectively. In search of the domain boundary, we found that the structures of nanopore and bilayer form concentric circles. The width of the latter is about one-fifth the diameter of the former. The section profiles across the domains (Fig. 3) show that molecules in the bilayer bear a taller apparent height than those in the monolayer and nanopores. Also discernible is the repositioning of molecules at the top layer after 10 imaging frames. Gradually the bilayer structure becomes nanoporous. The use of 1 μM and 0.1 mM tetrabutylammonium perchlorate also makes the domain sizes of nanopores smaller to 150 nm and 60 nm, respectively. The presence of charged electrolytes shields the electrical field and leads to a less significant degree of molecular polarisation. The electrolytes also develop a potential drop between the tip and substrate, diminishing the surface area which is able to afford an effective local charge strong enough to attract the polarised molecules onto the substrate. Overall, the dependence of domain size on the strength of the electrical field as well as the assembly taking place proximal to the tip support the hypothesis that the electrical field emitted *via* the tip enables the deposition of molecules.

In conclusion, we have demonstrated that electrical stimuli can reversibly deposit/desorb molecules onto a bare and monolayer substrate to build a molecular assembly beyond two dimensions. Applying a voltage pulse in the **1**-containing solution triggers the formation of hexagonal monolayers, bilayers, and honeycomb nanopores. Thus-prepared structures exhibit domain sizes of about 500 nm which can be reduced and hence be determined with the control experiments that activate pulses at lifted tip–substrate distances and in environments composed of electrolytes. The assembly is ascribed to electrical field-induced polarisation of **1** and the redistribution of local charge at the solid–liquid interface upon electrical stimuli. The difference in structures prepared by 4 V and 5 V pulses is attributed to the effective charge present over the saturated alkoxy chains of the first layer. The controllable formation of nanoporous networks of **1** offers a new template for supramolecular chemistry to evolve further.

We thank NSC (ROC) for financial support. Thanks also to Mr Min-Jie Huang (NTU) for insightful discussion.

Notes and references

1 (*a*) J. A. A. W. Elemans, S. Lei and S. De Feyter, *Angew. Chem., Int. Ed.*, 2009, **48**, 7298; (*b*) Y. Yang and C. Wang, *Chem. Soc. Rev.*, 2009, **38**, 2576.
2 D. Wang, L.-J. Wan and C.-L. Bai, *Mater. Sci. Eng., R*, 2010, **70**, 169.
3 S.-S. Li, B. H. Northrop, Q.-H. Yuan, L.-J. Wan and P. J. Stang, *Acc. Chem. Res.*, 2008, **42**, 249.
4 (*a*) Y. Wei, W. Tong and M. B. Zimmt, *J. Am. Chem. Soc.*, 2008, **130**, 3399; (*b*) K. E. Plass, A. L. Grzesiak and A. J. Matzger, *Acc. Chem. Res.*, 2007, **40**, 287.
5 R. van Hameren, P. Schön, A. M. van Buul, J. Hoogboom, S. V. Lazarenko, J. W. Gerritsen, H. Engelkamp, P. C. M. Christianen, H. A. Heus, J. C. Maan, T. Rasing, S. Speller, A. E. Rowan, J. A. A. W. Elemans and R. J. Nolte, *Science*, 2006, **314**, 1433.
6 A. Tracz, J. K. Jeszka, M. D. Watson, W. Pisula, K. Müllen and T. Pakula, *J. Am. Chem. Soc.*, 2003, **125**, 1682.
7 (*a*) S.-L. Lee, C.-Y. J. Chi, M.-J. Huang, C.-h. Chen, C.-W. Li, K. Pati and R.-S. Liu, *J. Am. Chem. Soc.*, 2008, **130**, 10454; (*b*) S.-L. Lee, N.-T. Lin, W.-C. Liao, C.-h. Chen, H.-C. Yang and T.-Y. Luh, *Chem.–Eur. J.*, 2009, **15**, 11594.
8 S. Yoshimoto, T. Sawaguchi, W. Su, J. Jiang and N. Kobayashi, *Angew. Chem., Int. Ed.*, 2007, **46**, 1071.
9 A. Ciesielski and P. Samorì, *Nanoscale*, 2011, **3**, 1397.
10 Y.-T. Shen, K. Deng, X.-M. Zhang, W. Feng, Q.-D. Zeng, C. Wang and J. R. Gong, *Nano Lett.*, 2011, **11**, 3245.
11 (*a*) Q. H. Wang and M. C. Hersam, *Nano Lett.*, 2011, **11**, 589; (*b*) H. Yanagi, K. Ikuta, H. Mukai and T. Shibutani, *Nano Lett.*, 2002, **2**, 951.
12 (*a*) S. Lei, K. Deng, Y.-L. Yang, Q.-D. Zeng, C. Wang and J.-Z. Jiang, *Nano Lett.*, 2008, **8**, 1836; (*b*) K. S. Mali, D. Wu, X. Feng, K. Müllen, M. Van der Auweraer and S. De Feyter, *J. Am. Chem. Soc.*, 2011, **133**, 5686; (*c*) L. Xu, X. Miao, X. Ying and W. Deng, *J. Phys. Chem. C*, 2012, **116**, 1061; (*d*) M. Li, K. Deng, Y.-L. Yang, Q.-D. Zeng, M. He and C. Wang, *Phys. Rev. B*, 2007, **76**, 155438.
13 (*a*) R. Xie, Y. Song, L. Wan, H. Yuan, P. Li, X. Xiao, L. Liu, S. Ye, S. Lei and L. Wang, *Anal. Sci.*, 2011, **27**, 129; (*b*) S. P. Sullivan, A. Schnieders, S. K. Mbugua and T. P. Beebe, Jr., *Langmuir*, 2005, **21**, 1322; (*c*) D. Takajo, Y. Okawa, T. Hasegawa and M. Aono, *Langmuir*, 2007, **23**, 5247.
14 S.-L. Lee, H.-A. Lin, Y.-H. Lin, H.-H. Chen, C.-T. Liao, T.-L. Lin, Y.-C. Chu, H.-F. Hsu, C.-h. Chen, J.-J. Lee, W.-Y. Hung, Q.-Y. Liu and C. Wu, *Chem.–Eur. J.*, 2011, **17**, 792.
15 S.-L. Lee, M.-J. Huang, C.-h. Chen, C.-I. Wang and R.-S. Liu, *Chem.–Asian J.*, 2011, **6**, 1181.

